Journal of Biomechanics 46 (2013) 1801–1809

Contents lists available at SciVerse ScienceDirect

Journal of Biomechanics

journal homepage: www.elsevier.com/locate/jbiomech
www.JBiomech.com

Computational fluid dynamics modelling of cerebrospinal fluid pressure in Chiari malformation and syringomyelia

Elizabeth C. Clarke [a,*], David F. Fletcher [b], Marcus A. Stoodley [c], Lynne E. Bilston [d]

[a] Murray Maxwell Biomechanics Laboratory, Kolling Institute of Medical Research, Sydney Medical School, University of Sydney, Level 10, Kolling Building 6, RNS Hospital, St Leonards, NSW 2065, Australia
[b] School of Chemical and Biomolecular Engineering, University of Sydney, Australia
[c] The Australian School of Advanced Medicine, Macquarie University, Australia
[d] Neuroscience Research Australia and Prince of Wales Clinical School, University of New South Wales, Australia

ARTICLE INFO

Article history:
Accepted 20 May 2013

Keywords:
Syringomyelia
Chiari malformation
Cerebrospinal fluid (CSF)
Computational fluid dynamics (CFD)
Magnetic resonance imaging (MRI)

ABSTRACT

The pathogenesis of syringomyelia in association with Chiari malformation (CM) is unclear. Studies of patients with CM have shown alterations in the CSF velocity profile and these could contribute to syrinx development or enlargement. Few studies have considered the fluid mechanics of CM patients with and without syringomyelia separately. Three subject-specific CFD models were developed for a normal participant, a CM patient with syringomyelia and a CM patient without syringomyelia. Model geometries, CSF flow rate data and CSF velocity validation data were collected from MRI scans of the 3 subjects. The predicted peak CSF pressure was compared for the 3 models. An extension of the study performed geometry and flow substitution to investigate the relative effects of anatomy and CSF flow profile on resulting spinal CSF pressure. Based on 50 monitoring locations for each of the models, the CM models had significantly higher magnitude ($p < 0.01$) peak CSF pressure compared with normal. When using the same CSF input flow waveform, changing the upper spinal geometry changed the magnitude of the CSF pressure gradient, and when using the same upper spinal geometry, changing the input flow waveform changed the timing of the peak pressure. This study may assist in understanding syringomyelia mechanisms and relative effects of CSF velocity profile and spinal geometry on CSF pressure.

1. Introduction

Chiari malformation Type I (CM) is an abnormality characterised by protrusion of the cerebellar tonsils through the foramen magnum. Approximately two thirds (Pinna et al., 2000) of patients with CM also develop syringomyelia, where fluid filled cysts (syrinxes) develop in the spinal cord. Many patients report headaches, pain, and motor and sensory disturbances. Surgery is the only available treatment but syrinxes may persist or enlarge after surgery, and it is not clear why some patients with CM develop syringomyelia and others do not. Understanding the mechanisms of syringomyelia has the potential to improve treatment for these patients.

Early theories of syrinx development in CM proposed that herniation of the cerebellar tonsils causes increased resistance across the foramen magnum thereby preventing spinal cord extracellular fluid outflow or driving fluid into the central canal (Heiss et al., 1999; Oldfield et al., 1994; Olivero and Dinh, 1992). However a syrinx may be under high pressure and it is not clear how the CSF would accumulate in the central canal against a pressure gradient. Another theory proposes that syringomyelia develops passively as a result of the Venturi effect, where narrowed regions of the CSF pathway result in higher velocity and lower pressure (Greitz, 2006), however clinical studies of CM patients have reported significant reductions in syrinx size following surgery without significant reduction in CSF velocity near the syrinx (Mauer et al., 2011), and the velocity of the fluid flow is low, so such an effect is likely to be small. Experimental studies have demonstrated that fluid flows into the cord and syrinx via the perivascular spaces (Rennels et al., 1990; Rennels et al., 1985; Stoodley et al., 1996). It is possible that the pressure gradient and/or timing of arterial pulsation-dependent CSF flow could be a driving force of syrinx fluid from the perivascular spaces into the central canal. A recent computational simulation demonstrated that even a moderate shift in the timing of the CSF pressure pulse relative to arterial pulse could influence the mass flow rate of CSF into the perivascular spaces (Bilston et al., 2010). More recently, a follow up study by Elliott et al. demonstrated that this mechanism requires that the spinal cord have non-zero compliance with the vascular bed (Elliott et al., 2011).

While MRI scanning can provide structural anatomical, velocity and flow rate data, and has been used to demonstrate the contribution

* Corresponding author. Tel.: +61 299 264821; fax: +61 299 265266.
E-mail address: elizabeth.clarke@sydney.edu.au (E.C. Clarke).

0021-9290/$ - see front matter © 2013 Elsevier Ltd. All rights reserved.
http://dx.doi.org/10.1016/j.jbiomech.2013.05.013

of arterial and venous pulsations to CSF pulsation (Bhadelia et al., 1997), it is not possible to measure non-invasively spinal CSF pressures in humans. Invasive CSF pressure measurements in patients with CM have demonstrated dissociation between cranial and spinal CSF pressures (Williams, 1981a; Williams, 1981b), and increased CSF pressure in CM patients that reduced following posterior fossa decompression surgery (Heiss et al., 1999). However these studies did not compare patients with and without syringomyelia and did not investigate any temporal changes in the CSF waveform (e.g. delays in peak CSF pressure or delays in onset of systolic flush). A very recent study by Heiss et al. has compared CSF pressures in CM patients with and without syringomyelia (Heiss et al., 2012). Subject-specific computational simulations provide an opportunity to non-invasively study CSF pressure in patients with CM, with and without syringomyelia. Previous computational simulations of the spinal subarachnoid space (SSAS) have investigated the mechanisms of syrinx development in conditions such as arachnoiditis, finding that a porous obstruction in the SSAS changes timing and magnitude of peak CSF pressure (Cheng et al., 2012). Another study used computational modelling to investigate the effect of tonsillar herniation on CSF pressure by extending normal tonsil geometry inferiorly, finding that modified tonsil geometry increased the CSF pressure gradient (Linge et al., 2011). To our knowledge this is the first study to investigate the cyclic CSF pressure profile using subject-specific models of Chiari patients with and without syringomyelia.

2. Methods

2.1. MRI scanning and flow measurements

The University of NSW Human Research and Ethics Committee approved all experimental protocols, and all participants gave written informed consent to enter the study. Three participants underwent MRI scanning of the head and neck; one patient with CM and syringomyelia (female, 58 years, 80 kg), one patient with CM but no syringomyelia (female, 60 years, 65 kg), and one healthy control subject (female, 60 years, 80 kg).

A 3D sagittal isotropic (0.94 mm) T1-weighted turbo field echo MRI of the head and neck, and cardiac-gated cine phase-contrast (PC) MRI scans were performed using a 3 T MRI scanner (Philips Achieva TX, Best, Netherlands). The parameters for the 3D isotropic MRI scan were flip angle=8°, matrix=288 × 288, FOV=270 × 270 × 169, TR/TE=5.5/2.4 m s, slice thickness=0.94 mm. For the PC-MRI scans, retrospective cardiac gating was achieved using VCG leads, and 30 cardiac phase images were collected, measured from the onset of the R wave. PC-MRI scans were performed at the following cranial/spinal levels and encoding velocities (V_{enc}) using an (axial) scan plane aligned perpendicular to the CSF flow: 5 mm cranial to the tip of the cerebellar tonsils (V_{enc} 10 cm/s); mid-vertebral C2 (V_{enc} 9 cm/s); and mid-vertebral C5 (V_{enc} 13 cm/s) (Fig. 1A). The spatial resolution of the PC-MRI scans was 0.694–0.977 mm^2. Encoding velocities were determined during pilot studies in order to prevent aliasing. Other typical PC-MRI parameters were flip angle=10°, matrix=240 × 176, FOV=250 × 250, TR/TE=21/6.8 m s, slice thickness=5 mm.

CSF velocity and flow rate were measured from PC-MRI scans using the freely available analysis software Segment (Heiberg et al., 2010). For the tonsil-level scan the entire CSF cross-section was segmented and analysed for flow rate data (Fig. 1D and E), and for the C2- and C5-level scans velocity data were analysed using 10 regions of interest (2 mm diameter) spaced evenly around the SSAS (Fig. 1B and C). The tonsil-level flow rate was represented by a 6th order Fourier series for use as a flow input function for the models (Fig. 5B), and the C2 and C5 velocity data were used for model validation (Fig. 3).

2.2. Computational modelling

The spinal cord, spinal canal and cerebellum were segmented manually from the 3D MRI scans using SURFdriver software. These point cloud segmentations were imported into Rhinoceros (v3.0, Robert McNeal and associates, WA) and fitted with closed non-rational B-splines of degree 3 passing through the points for smoothing. These were then fitted with a surface (loft) and capped to create volumes. The CSF volume was created by Boolean subtraction of the cerebellum and spinal cord volumes from the spinal canal volume, then trimmed 5 mm cranial to the base of the cerebellar tonsils and 95 mm caudal to the base of the tonsils (Fig. 2A). The cranial end of the CSF volume was extended upwards by 5 mm to

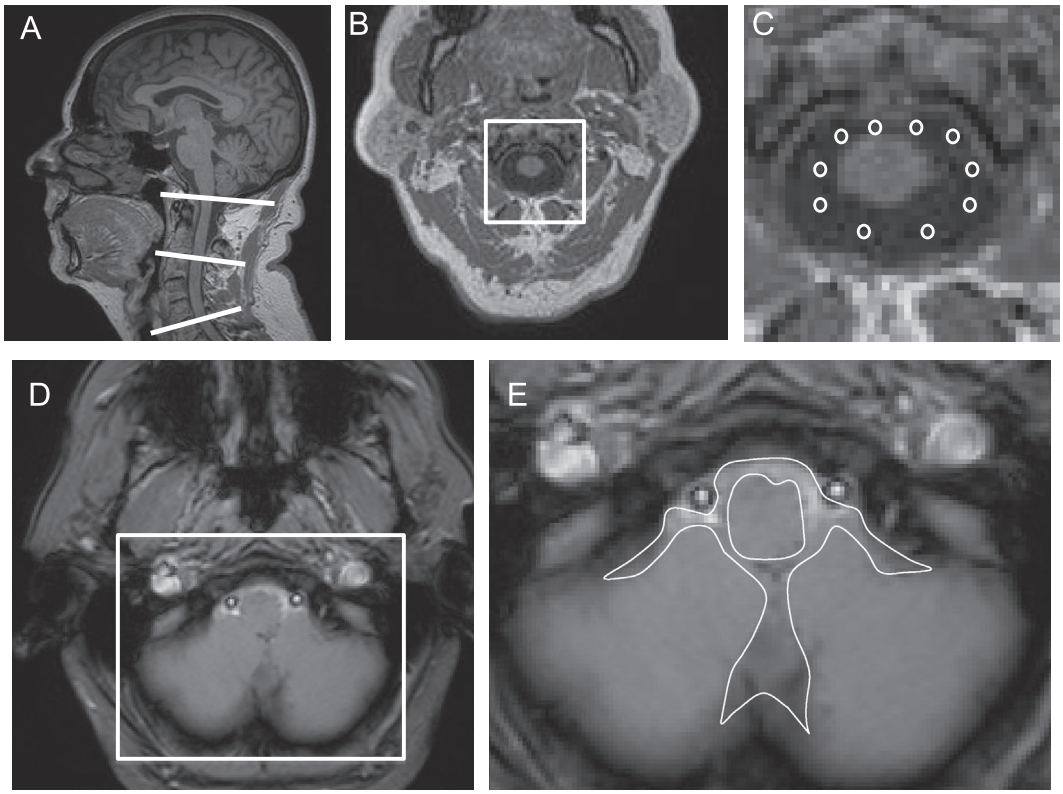

Fig. 1. Example MRI scans from a healthy control volunteer showing (A) the approximate alignment of the cine phase-contrast MRI scan planes (cerebellar tonsils, mid-C2 and mid-C5) aligned perpendicular to the CSF flow, (B) an example anatomical scan through the mid-C2, (C) a magnified view of a mid-C2 level phase image (as indicated in B) depicting approximate locations of the 10 regions used for validation of the models against MRI-measured CSF velocity data, (D) an example anatomical scan through the cerebellar tonsil level, and (E) a magnified view of a tonsil level phase image (as indicated in D) depicting manual segmentation of the entire CSF region.